ORIGINAL PAPER

Ab initio calculations of molecular properties of low–lying electronic states of 2–cyclopenten–1–one – link with biological activity

Jana Fišanová · Ivan Černušák · Vladimír Kellö

Abstract Geometries, vibrational frequencies, vertical and adiabatic excitation energies, dipole moments and dipole polarizabilities of the ground and the three lowest electronic excited states, $S_1(n, \pi^*)$, $T_1(n, \pi^*)$, and $T_2(\pi, \pi^*)$ of the 2–cyclopenten–1–one molecule (2CP) were calculated at the CCSD and CCSD(T) levels of approximation. Our results indicate that two triplets $T_1(n, \pi^*)$ and $T_2(\pi, \pi^*)$ are lying very close each to other, while the singlet $S_1(n, \pi^*)$ is well above them. There are dramatic changes in dipole moments for (n, π^*) excited states in respect to the ground state. On the other hand the $T_2(\pi, \pi^*)$ state has a similar dipole moment as the ground state. These changes can be interpreted within the MO picture using electrostatic potential maps and changes in model IR spectra. Our CCSD(T) dipole moment data for the ground state and almost isoenergetic triplets $T_1(n, \pi^*)$ and $T_2(\pi, \pi^*)$ are 1.469 a.u., 0.551 a.u., and 1.124 a.u., respectively. Dipole polarizabilities of investigated excited states are much less affected by electron excitations than dipole moments. These are the first dipole moment and polarizability data of 2CP in the literature. The changes of molecular properties upon excitation to $S_1(n, \pi^*)$ and $T_1(n, \pi^*)$ correlate with the experimental data on the biological activity of 2CP related to the α, β–unsaturated carbonyl group.

J. Fišanová · I. Černušák · V. Kellö (✉)
Department of Physical and Theoretical Chemistry,
Faculty of Natural Sciences, Comenius University,
Mlynska dolina,
SK–842 15 Bratislava, Slovakia
e-mail: kelloe@fns.uniba.sk

J. Fišanová
e-mail: palenikova.jana@gmail.com

I. Černušák
e-mail: cernusak@fns.uniba.sk

Introduction

Electric properties, like dipole moments and polarizabilities of molecules in excited electronic states are known much less than excitation energies or relaxed geometries. This observation applies equally to experimental works and theoretical calculations and it is completely valid also in the case of the 2–cyclopenten–1–one molecule (2CP).

Permanent dipole moments of small molecules in excited states might be experimentally obtained by high–resolution laser–induced fluorescence spectroscopy observing Stark shifts in the presence of static electric fields, see e.g., recent papers of Steimle et al. [1, 2] and see also reviews on Stark spectroscopy by Boxer et al. [3, 4].

Dipole moments and polarizabilities of molecules in excited states are closely related to solvent effects on frequency shifts in electronic spectra. Changes in dipole moments of molecules due to electronic excitations have a central role in frequency shifts. The source of these solvatochromic shifts is interpreted in terms of electrostatic and dispersion interactions between the solute and solvent molecules, which are different in the ground and excited state. Very recently Pašteka et al. [5] published a theoretical paper on electric properties of the acetone molecule in electronic excited states, giving a very good and concise insight into this topic.

During the past four decades a number of papers appeared studying the S_0 ground and $S_1(n, \pi^*)$, $T_1(n, \pi^*)$, and $T_2(\pi, \pi^*)$ excited electronic states of 2CP experimentally [6–11], and

also theoretically [12–16]. These studies were mainly aimed at excitation energies and vibration frequencies, however, we did not find any information about dipole moments and polarizabilities of 2CP in the literature. Thus, the purpose of this paper is mainly focused on theoretical calculations of these properties using highly sophisticated electron correlation methods.

2CP recently also became a subject of intensive medicinal research. Being a highly water soluble small molecule, 2CP could be an ideal candidate to overcome pharmacological issues related to drug delivery and penetration. Its cytotoxic activity was tested on various melanoma and lung cancer cells. Rossi et al. [17] have reported that 2CP controls the expression of the heat shock proteins, Ianaro et al. [18] have shown that 2CP can have therapeutic relevance for the prevention of human restenosis and Rosetri et al. [19] investigated the cytotoxicity against cancer cells of the model compound 2-cyclopenten-1-one. Several authors also investigated the synthesis of various derivatives of 2CP with the aim to produce efficient precursors for pharmaceutical use [20–22]. One of the key properties of 2CP indicated in these papers is the presence of the α, β–unsaturated carbonyl group which is essential for triggering the heat shock transcription factor activation [17], in anti–inflammatory effects [18] or inhibition of nuclear factor kappa–light–chain–enhancer of activated B cells [22]. Modification of this bond upon excitation (by e.g., UV radiation) can affect biological activity of 2CP.

The aim of this paper is threefold:

- to reoptimize the geometries at the B3LYP and MP2 levels and predict their model harmonic IR spectra,
- interpret the importance of the α, β-unsaturated carbonyl group on molecular level analyzing the spectroscopic properties of 2CP,
- to provide an extended set of dipole moments and polarizabilities for the four lowest electronic states of 2CP which are reported here for the first time and might be helpful for developing solvation models related to pharmacological research.

Finally, we contribute to the (yet unfinished) discussion on the triplet states ordering, calculating vertical as well as adiabatic excitation energies.

Computational methods

In the present calculations we used several quantum chemical methods within two program packages, Gaussian03 [23] and MOLCAS7 [24]. Gaussian03 was exploited for geometry optimizations and calculating vibrational frequencies using the B3LYP and MP2 methods. MOLCAS7 was

exploited for calculating excitation energies and electric properties using CASSCF [25] and coupled cluster CCSD and CCSD(T) methods based on restricted open–shell Hartree–Fock reference wave function [26, 27]. The open–shell singlets which cannot be described by a single–determinant reference wave function were calculated by the two–determinant CCSD method [28]. In this work we have utilized several basis sets. We performed geometry optimizations using the 6-311+G** [23] and cc-pVTZ [29] basis sets. Dipole moments and polarizabilities were calculated using Sadlej's Pol [30–32] and z2Pol [33] basis sets which were particularly developed for calculations of these properties. The polarized z2Pol and Pol basis sets were used also for excitation energies, however, in this case we relied more on Dunning's cc-pVTZ and mainly the cc-pVQZ [29] basis set. Since only the first row atoms are involved in 2CP, relativistic effects were neglected in this study [34].

The evaluation of components of the dipole moment and the dipole polarizability tensor was accomplished by using a numerical finite–field perturbation technique [35–37]. Numerical derivatives were obtained using the Romberg scheme [38, 39]. The external electric field strengths were set to 0.002, 0.004 and 0.008 a.u. These field strengths were carefully checked against the dipole moment expectation values at the CASSCF level.

Results and discussion

Geometries and vibrational frequencies

2-cyclopenten-1-one in its ground electronic state S_0, with conjugated double bonds, has the planar C_s symmetry. These bonds retain the conjugated character also in the excited singlet state $S_1(n, \pi^*)$ and consequently, the ring remains planar and the carbonyl group remains in the plane of the ring [40]. The excited triplet states $T_1(n, \pi^*)$ and $T_2(\pi, \pi^*)$ lack planar symmetry. B3LYP/6-311+G** calculations of Choo et al. [15] provides a tiny ring–puckering barrier of 8 cm^{-1} for the $T_1(n, \pi^*)$ state, while for the $T_2(\pi, \pi^*)$ state the barrier is 999 cm^{-1}. The experimental barrier to ring–puckering for the $T_1(n, \pi^*)$ state determined by Pillsbury et al. [10] is 43.5 cm^{-1}.

We have performed a full geometry optimization for all four electronic states of 2CP at the B3LYP/6-311+G** level and also using the MP2 method with the 6-311+G** and cc-pVTZ basis set. The calculated B3LYP/6-311+G** and MP2/cc-pVTZ geometries are depicted in Fig. 1. The corresponding rotational constants are presented in Table 1 and MP2/cc-pVTZ model IR spectra are collected in Fig. 2. For the ground state the matching of experimental [41] and scaled model IR spectra is very good. Our B3LYP/6-311+G** geometry data are just reproducing the results of Choo et al. [15], however, there are tiny differences in rotational

Fig. 1 Calculated geometries [Å] of 2-cyclopenten-1-one in its ground and excited states

B3LYP/6-311+G**   MP2/cc-pVTZ
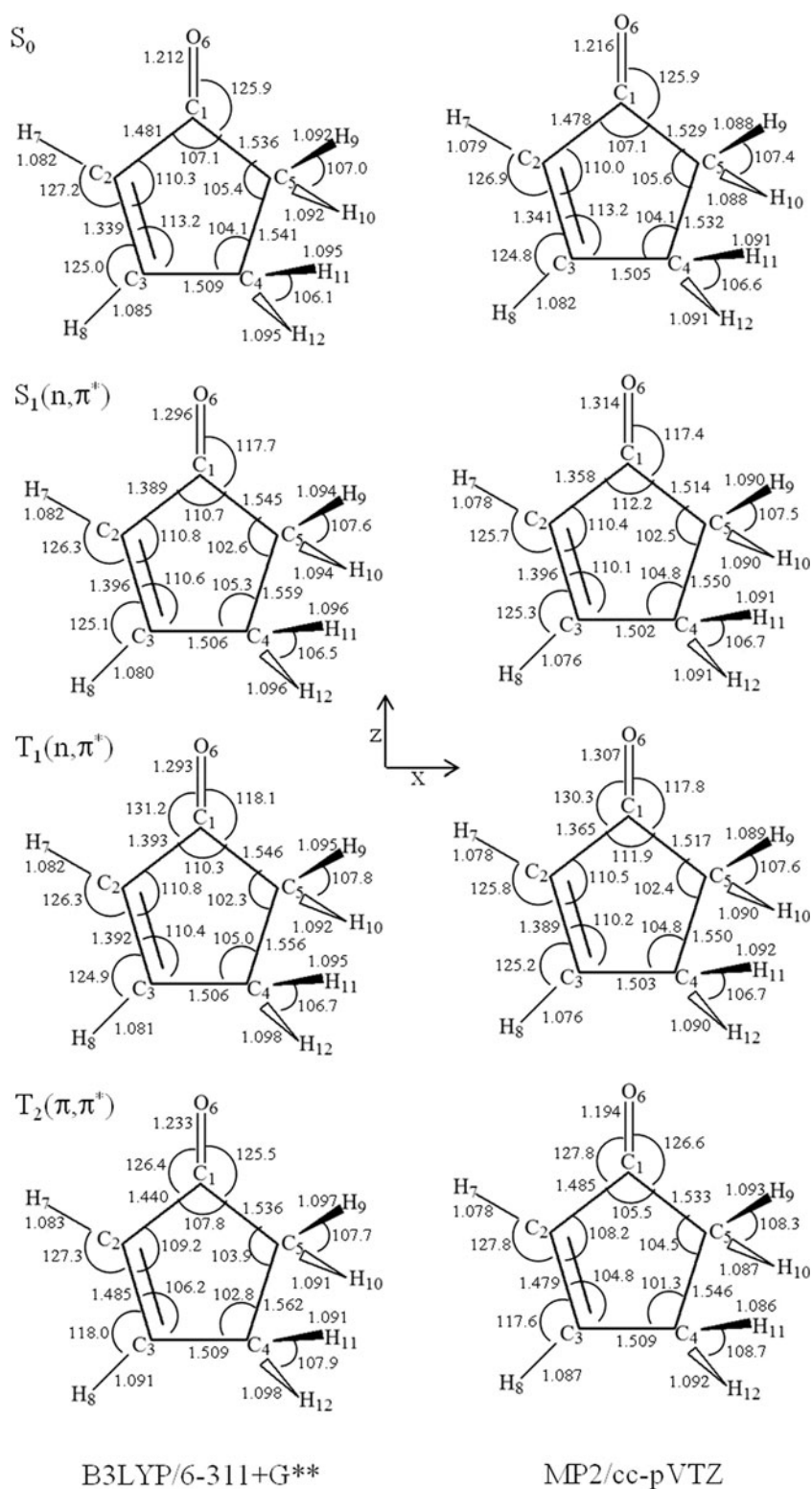
constants. A detailed discussion about changes in geometries of the four electronic states is presented by Choo et al. [15]. The essence of this discussion is an elongation of the C=O and C=C double bonds in the excited states and losing the planar symmetry in the case of triplets. The MP2/cc-pVTZ geometries do not differ much from B3LYP/6-311+G** ones, except the $T_2(\pi, \pi^*)$ state where the C=O bond is shorter by 0.1 Å and it is even shorter than for the ground state S_0. Thus, the MP2 C=O bond length exhibits opposite trend compared to B3LYP. Comparing the B3LYP/6-311+G** and MP2/cc-

Table 1 Rotational constants (GHz) of 2-cyclopenten-1-one

| State	Method	Basis set	A	B	C	ABC
S_0	B3LYP	6-311+G**	7.431	3.581	2.490	66.260
	B3LYP[a]	6-311+G**	7.434	3.581	2.491	66.313
	B3LYP	cc-pVTZ	7.463	3.594	2.500	67.055
	MP2	cc-pVTZ	7.478	3.590	2.500	67.115
	exp.[b]		7.410	3.586	2.493	66.245
$S_1(n, \pi^*)$	B3LYP	6-311+G**	7.439	3.516	2.460	64.343
	B3LYP[a]	6-311+G**	7.440	3.516	2.460	64.351
	B3LYP	cc-pVTZ	7.479	3.528	2.470	65.173
	MP2	cc-pVTZ	7.574	3.556	2.494	67.171
$T_1(n, \pi^*)$	B3LYP	6-311+G**	7.441	3.524	2.469	64.742
	B3LYP[a]	6-311+G**	7.442	3.524	2.469	64.751
	B3LYP	cc-pVTZ	7.472	3.532	2.472	65.239
	MP2	cc-pVTZ	7.557	3.564	2.497	67.252
$T_2(\pi, \pi^*)$	B3LYP	6-311+G**	7.422	3.481	2.516	65.003
	B3LYP[a]	6-311+G**	7.422	3.481	2.516	65.003
	B3LYP	cc-pVTZ	7.455	3.493	2.523	65.700
	MP2	cc-pVTZ	7.464	3.512	2.563	67.185

[a] From ref. [15]

[b] From ref. [9]

pVTZ rotational constants data we found almost no change in the ABC product for the S_0 state. In the case of excited states these changes in the ABC product amounted to 4 %, however, 3 % are due to the method itself and only 1 % due to the basis set.

For all four investigated electronic states of 2CP we calculated vibrational frequencies using the MP2 method and the cc-pVTZ basis set. *Ab initio* determined vibrational frequencies are often scaled by empirical factors. Irikura et al. published a detailed study on *ab initio* scaling factors for vibrational frequencies and their recommended factor for

Fig. 2 Model MP2/cc-pVTZ IR spectra of 2CP scaled frequencies, the relative intensities of the excited states were shifted by 50, 100, and 150 units. The S_0 experimental IR spectrum (dashed line) reproduced from the NIST data [41]

MP2/cc-pVTZ data is 0.9595 ± 0.0692 [42]. Based on the comparison of experimental and our harmonic frequencies for the S_0 state we used the scaling factor 0.978, except for the C–H stretching modes (larger than 3000 cm^{-1}) where 0.942 was utilized. This choice is in agreement with the cited recommendation. Our scaled MP2/cc-pVTZ vibrational frequencies are presented in Table 2 together with available experimental [6, 8] and B3LYP/6-311+G** data [15]. There are two important trends in IR spectra related to C=O and C=C bonds. The weakening of the C=C bond upon excitation is clearly visible in IR spectra, the pertinent modes are 1604 (S_0), 1353 (S_1), 1358 (T_1) and 1303 cm^{-1} (T_2), respectively. At the same time, the α, β-unsaturated carbonyl is significantly weakened from 1736 in S_0 to 1533 cm^{-1} (S_1) and 1513 cm^{-1} (T_1) but enhanced in T_2 (2122 cm^{-1}).

Experimental data for the excited electronic states remained rather patchy. There are only 13 known frequencies for the $S_1(n, \pi^*)$ state [8] and the situation for the non–planar states is even worse. Pillsbury et al. assigned four low–frequency modes for the $T_1(n, \pi^*)$ state [10, 11]. We did not find any experimental data for the $T_2(\pi, \pi^*)$ state. Agreement of our MP2 values with experimental ones for the ground state is very reasonable, the root mean square deviation is 11 cm^{-1}, and essentially of similar quality as B3LYP/6-311+G** data [15] with the root mean square deviation of 9 cm^{-1}. A similar claim may be said about $S_1(n, \pi^*)$ frequencies. Choo et al. [15] calculated vibrational frequencies of excited triplets in the C_s symmetry, while our calculations were performed in the puckered geometry of the C_1 symmetry, thus the comparison would be more complicated. We do not expect that the accuracy of vibrational frequencies for the triplets is considerably lower than for the singlets.
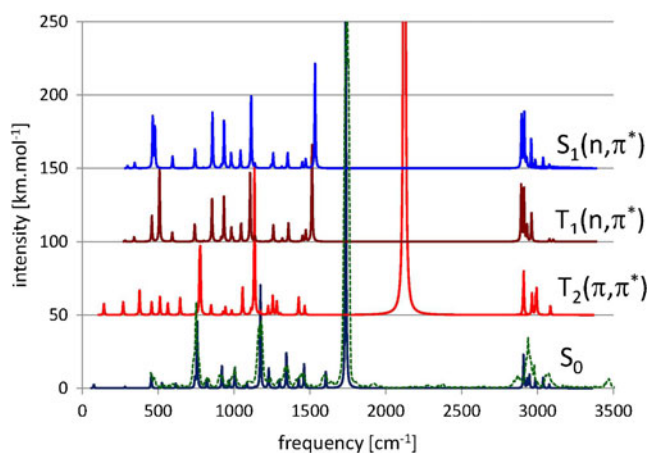
Excitation energies

We performed calculations of excitation energies in four different bases of atomic functions. We used two polarized basis sets z2Pol and Pol, which are dedicated to calculations of dipole moments and polarizabilities, just to illustrate how accurate excitation energies they may provide. However, in the case of energy we trust more in the cc-pVTZ and cc-pVQZ sets. Perhaps, it is worthwhile to mention the total number of contracted functions for the 2CP molecule. In the case of the z2Pol and Pol set it is 144 and 198, respectively. The cc-pVTZ and particularly cc-pVQZ basis is much larger, 264 and 528 functions, respectively. Calculations were carried out in geometries optimized at the B3LYP/6-311+G** level and also at the MP2/cc-pVTZ level.

Vertical excitation energies, T_e values, calculated in the S_0 ground state geometry, are presented in Table 3. The simplest method presented in Table 3, CASSCF, generates

Table 2 Vibrational frequencies (cm^{-1}) of 2-cyclopenten-1-one

No.[a]	S_0			$S_1(n, \pi^*)$			$T_1(n, \pi^*)$	$T_2(\pi, \pi^*)$
	MP2[b]	DFT[c]	exp.[d]	MP2[b]	DFT[c]	exp.[e]	MP2[b]	MP2[b]
1	3077	3090	3083	3104	3098		3103	3085
2	3037	3051	3067	3080	3080		3078	2994
3	2933	2940	2938	2912	2915		2960	2989
4	2908	2907	2885	2894	2884		2931	2963
5	1736	1750	1748	1533	1472	1418	2911	2909
6	1604	1616	1599	1472	1451	1357	2892	2904
7	1461	1461	1452	1449	1419		1513	2122
8	1425	1430	1418	1353	1368		1472	1465
9	1345	1346	1345	1314	1319		1450	1425
10	1299	1303	1305	1257	1258		1358	1303
11	1228	1239	1232	1243	1222		1317	1281
12	1174	1164	1173	1112	1058		1258	1254
13	1085	1093	1094	1042	1034	1037	1241	1224
14	1006	989	999	980	969	974	1209	1173
15	919	905	912	915	892	906	1137	1134
16	820	812	822	857	810	849	1106	1111
17	741	751	753	742	748	746	1046	1056
18	615	623	630	594	581	587	992	984
19	454	459	464	345	342	348	982	943
20	2985	2977	2980	2958	2948		933	928
21	2947	2928	2927	2929	2900		914	848
22	1220	1214	1208	1210	1189		854	778
23	1138	1142	1138	1137	1111		800	773
24	1003	1012	1007	990	977		740	644
25	968	975	960	934	854		592	563
26	812	815	815[f]	797	785	768	508	511
27	756	757	750[f]	478	491		457	456
28	524	534	537	463	416	422	341	377
29	281	291	287[f]	298	253	274	281	269
30	75	102	94[f]	18	25	67	35	142

[a] The number of vibrational mode. In the case of planar geometries of the S_0 and $S_1(n, \pi^*)$ state, modes 1–19 and 20–30 belong to the a′ and a″ representation, respectively

[b] Present work, the MP2 frequencies calculated in the cc-pVTZ basis set were scaled by 0.978, except for the C–H stretching modes (larger than 3000 cm^{-1}) where 0.942 was utilized

[c] From ref. [15], B3LYP/6-311+G** frequencies scaled by 0.985, except for the C–H stretching modes (larger than 3000 cm^{-1}) where 0.964 was utilized

[d] From ref. [6] unless otherwise noted

[e] From ref. [8]

[f] Experimental frequencies from ref. [7] and reassigning from ref. [15]

reference wave function for coupled cluster calculations. It represents just HF for the closed–shell ground state, and just two active electrons in two orbitals for open–shell excited states. The data of Table 3 indicate that the electron correlation contribution to excitation energies is by no means negligible, about 0.6 eV which is 15 % of the total value.

Table 3 Vertical excitation energies (eV) of 2-cyclopenten-1-one[a]

State	Method	z2Pol	Pol	cc-pVTZ	cc-pVQZ
		geometry B3LYP/6-311+G**			
$S_1(n, \pi^*)$	CASSCF	3.364	3.628		
	CCSD	3.816	4.009		
$T_1(n, \pi^*)$	CASSCF	3.091	3.290		
	CCSD	3.633	3.661		
	CCSD(T)	3.674	3.693		
$T_2(\pi, \pi^*)$	CASSCF	3.465	3.500		
	CCSD	4.108	4.053		
	CCSD(T)	4.165	4.137		
		geometry MP2/cc-pVTZ			
$S_1(n, \pi^*)$	CASSCF	3.320	3.583	3.505	3.500
	CCSD	3.790	3.982	3.824	3.835
$T_1(n, \pi^*)$	CASSCF	3.052	3.249	3.238	3.238
	CCSD	3.607	3.635	3.618	3.638
	CCSD(T)	3.651	3.670	3.672	3.692
$T_2(\pi, \pi^*)$	CASSCF	3.441	3.477	3.491	3.487
	CCSD	4.080	4.026	4.029	4.028
	CCSD(T)	4.137	4.111	4.128	4.129
		other data[b]			
$T_1(n, \pi^*)$	B3LYP		3.38		
	CIS(D)		3.69		
$T_2(\pi, \pi^*)$	B3LYP		3.84		
	CIS(D)		4.23		

[a] T_e values

[b] From ref. [13]

The contribution from triple excited configurations is up to 0.1 eV. The $S_1(n, \pi^*)$ state, which cannot be described by a single–determinant wave function, was calculated by the two–determinant CCSD method implemented in MOL-CAS7 [24] and this implementation does not have the CCSD(T) option available.

The sequence of vertical excitation energies of 2CP molecule is $T_1(n, \pi^*)$, $S_1(n, \pi^*)$, and the highest one is $T_2(\pi, \pi^*)$. The shifts in energies due to replacing the B3LYP/6-311+G** geometry by MP2/cc-pVTZ one are very small, up to 0.02 eV. The effect due to increasing size of the basis set is also rather small here. The polarized Pol basis set provides values differing by 0.02 eV from much larger cc-pVQZ set, and even z2Pol data are not much worse. As a reference, we found only B3LYP and CIS(D) calculations of 2CP vertical excitation energies for the $T_1(n, \pi^*)$ and $T_2(\pi, \pi^*)$ state by Sunoj et al. [13], and these values are very similar to ours.

Calculated adiabatic excitation energies, T_e and also T_0 values are presented in Table 4. The electron correlation effect in adiabatic excitation energies is larger than in the case of vertical ones, amounts up to 0.8 eV which represents 25 % of the total value. Contributions coming from triple excited configurations into adiabatic and vertical excitation

Table 4 Adiabatic excitation energies (eV) of 2-cyclopenten-1-one[a]

State	Method	z2Pol	Pol	cc-pVTZ	cc-pVQZ
			geometry B3LYP/6-311+G**		
$S_1(n, \pi^*)$	CASSCF	2.529	2.936		
	CCSD	3.080	3.467		
$T_1(n, \pi^*)$	CASSCF	2.479	2.802		
	CCSD	2.969	3.197		
	CCSD(T)	3.004	3.232		
$T_2(\pi, \pi^*)$	CASSCF	2.438	2.527		
	CCSD	2.941	3.026		
	CCSD(T)	2.999	3.106		
			geometry MP2/cc-pVTZ		
$S_1(n, \pi^*)$	CASSCF	2.414	2.832	2.760	2.774
	CCSD	3.113	3.485	3.345, 3.273[b]	3.379, 3.307[b]
$T_1(n, \pi^*)$	CASSCF	2.374	2.708	2.706	2.721
	CCSD	3.006	3.220	3.222	3.261
	CCSD(T)	3.061	3.279	3.304, 3.232[b]	3.345, 3.273[b]
$T_2(\pi, \pi^*)$	CASSCF	2.473	2.447	2.498	2.500
	CCSD	3.106	3.068	3.183	3.202
	CCSD(T)	3.178	3.167	3.302, 3.242[b]	3.325, 3.265[b]
			other data		
$S_1(n, \pi^*)$	B3LYP		3.109[c]		
	CIS(D)		3.51[d]		
	expt.		3.374[e], 3.374[f]		
$T_1(n, \pi^*)$	MP3		3.22[g]		
	IMOMO CCSD(T):MP2		3.11[g]		
	CASSCF		3.25[h]		
	B3LYP		3.037[c], 3.02[i]		
	expt.		3.218[f]		
$T_2(\pi, \pi^*)$	MP3		3.13[g]		
	IMOMO CCSD(T):MP2		3.01[g]		
	CASSCF		3.08[h]		
	B3LYP		3.067[c], 3.03[i]		
	expt.		3.257[f]		

[a] T_e values, if not otherwise noted

[b] T_0 value, ZPE correction at MP2/cc-pVTZ level included

[c] From ref. [15]

[d] T_0 value, from ref. [16]

[e] T_0 value, from ref. [8]

[f] T_0 value, from ref. [11]

[g] From ref. [12]

[h] From ref. [14]

[i] From ref. [13]

energies are comparable. Our comments about the used basis sets and the choice of geometries presented for vertical excitation energies apply also for adiabatic ones. The zero point energy (ZPE) corrections to electronic adiabatic excitation energies based on our calculated MP2/cc-pVTZ vibration frequencies, Table 2, are -0.072 eV, -0.072 eV, and -0.060 eV for the states $S_1(n, \pi^*)$, $T_1(n, \pi^*)$, and $T_2(\pi, \pi^*)$, respectively.

The sequence of adiabatic excitation energies is different than it is for vertical ones. All our and other calculations from the literature, as well as all experiments place the $S_1(n, \pi^*)$ state as the highest one. However, order of the triplets is ambiguous. Let us compare our CCSD(T) energies calculated in MP2/cc-pVTZ geometries. In the z2Pol basis we got the $T_2(\pi, \pi^*)$ state higher than $T_1(n, \pi^*)$ by more than 0.1 eV, while for larger Pol basis it is opposite. The polarized basis sets are certainly not aimed for the energetics and it would be unwise to draw any firm conclusions based on these data. In the cc-pVTZ set with the included ZPE correction the $T_2(\pi, \pi^*)$ state is higher by 0.01 eV, while in the cc-pVQZ set it is lower by less than 0.01 eV. Similar ambiguities may be found in the literature. Morokuma et al. [12] using the standard MP3 method and the integrated molecular orbital + molecular orbital IMOMO CCSD(T):MP2 method placed $T_1(n, \pi^*)$ by 0.01 eV above $T_2(\pi, \pi^*)$. A similar order was obtained by Garcia–Exposito et al. [14] using the CASSCF method and the 6-31G* basis set. On the other hand, phosphorescence excitation spectroscopy [11], suggested that $T_2(\pi, \pi^*)$ is above $T_1(n, \pi^*)$ by 0.04 eV. This order is supported also by B3LYP calculations of Choo et al. [15] and Sunoj et al. [13] with the differences of 0.03 eV and 0.02 eV, respectively. To summarize a bit, the difference between $T_1(n, \pi^*)$ and $T_2(\pi, \pi^*)$ is a rather sensitive quantity. Although our CCSD(T)/cc-pVQZ data represent a very solid level of computational accuracy, we feel that it is still not possible to resolve which of the triplets is higher. We can just conclude that the states $T_1(n, \pi^*)$ and $T_2(\pi, \pi^*)$ are nearly isoenergetic.

Both the vertical and adiabatic excitation energies refer to wavelengths on the upper edge of the UV-A radiation (330-370 nm). According to Pillsbury et al. [11] the most intense is the $S_1(n, \pi^*) \leftarrow S_0$ transition, followed by weaker $T_1(n, \pi^*) \leftarrow S_0$, while the $T_2(\pi, \pi^*) \leftarrow S_0$ is strongly spin–forbidden. Our CCSD and CCSD(T) excitation energies (vertical in Table 3 and adiabatic in Table 4) indicate that the biological activity of 2CP can be affected by the common UV–radiation present in our environment and significantly weakened in the states $S_1(n, \pi^*)$ and $T_1(n, \pi^*)$.

Dipole moments and polarizabilities

Calculated dipole moments are presented in Table 5. They were calculated in two basis sets particularly designed for calculations of molecular properties. The 'small' z2Pol [33] and the 'standard' Pol set [30–32] provide qualitatively same values of the dipole moment with differences up to 0.1 a.u. There are very small differences (0.03 a.u.), for the $S_1(n, \pi^*)$ and $T_1(n, \pi^*)$ states between 'vertical' dipole moments, calculated in the ground state S_0 geometry, and 'adiabatic' ones, calculated in the given excited state geometry. In the case of the $T_2(\pi, \pi^*)$ state this difference is larger

Table 5 Dipole moments (a.u.) of 2-cyclopenten-1-one[a]

State	Method	Basis z2Pol				Basis Pol			
		μ_x	μ_y	μ_z	$|\mu|$	μ_x	μ_y	μ_z	$|\mu|$
'Vertical'[b]									
S_0	CASSCF	-0.122	0.000	-1.797	1.801	-0.112	0.000	-1.764	1.767
	CCSD	-0.085	0.000	-1.509	1.511	-0.084	0.000	-1.494	1.496
	CCSD(T)	-0.081	0.000	-1.507	1.509	-0.078	0.000	-1.467	1.469
$S_1(n, \pi^*)$	CASSCF	-0.204	0.000	-0.576	0.611	-0.227	0.000	-0.427	0.483
	CCSD	-0.284	0.000	-0.695	0.751	-0.307	0.000	-0.561	0.639
$T_1(n, \pi^*)$	CASSCF	-0.196	0.000	-0.532	0.567	-0.214	0.000	-0.404	0.457
	CCSD	-0.283	0.000	-0.592	0.656	-0.300	0.000	-0.479	0.565
	CCSD(T)	-0.297	0.000	-0.598	0.667	-0.315	0.000	-0.489	0.582
$T_2(\pi, \pi^*)$	CASSCF	0.055	0.000	-1.652	1.653	0.060	0.000	-1.646	1.647
	CCSD	0.064	0.000	-1.430	1.431	0.063	0.000	-1.418	1.419
	CCSD(T)	0.060	0.000	-1.405	1.406	0.059	0.000	-1.377	1.378
'Adiabatic'[c]									
$S_1(n, \pi^*)$	CASSCF	-0.281	0.000	-0.529	0.599	-0.286	0.000	-0.439	0.524
	CCSD	-0.264	0.000	-0.646	0.698	-0.278	0.000	-0.535	0.603
$T_1(n, \pi^*)$	CASSCF	-0.298	0.015	-0.478	0.564	-0.301	0.014	-0.387	0.490
	CCSD	-0.288	0.018	-0.557	0.628	-0.295	0.017	-0.454	0.542
	CCSD(T)	-0.297	0.019	-0.560	0.634	-0.302	0.017	-0.461	0.551
$T_2(\pi, \pi^*)$	CASSCF	-0.191	0.068	-1.356	1.371	-0.180	0.071	-1.334	1.348
	CCSD	-0.189	0.036	-1.135	1.151	-0.183	0.040	-1.108	1.124
	CCSD(T)	-0.193	0.033	-1.116	1.133	-0.188	0.034	-1.107	1.124

[a] MP2/cc-pVTZ geometries used, 1 a.u. 0 2.541 746 D = $8.478353 \cdot 10^{-30}$ Cm
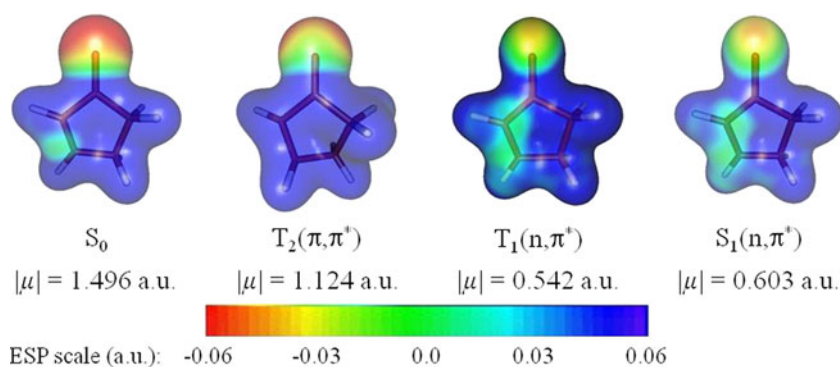
[b] Geometries of the ground state

[c] Geometries of the given state

(0.25 a.u.) due to a larger geometrical distortion from the planar symmetry. The (n, π^*) excitation caused a dramatic decrease of the dipole moment, up to one third of the ground state value, both for the singlet and triplet state. Excitation of the oxygen lone pair electron to the ring effectively shortened the dipole and that is the explanation of the dipole moment decrease. On the other hand, the (π, π^*) excitation brings much smaller reduction of the dipole moment. We found previously for H_2O and H_2S [43] similar large changes of the dipole moment of excited states. The fact that two nearly isoenergetic triplets have radically different dipole moments is very striking.

The differences in dipole moments can be alternatively interpreted in terms of isodensity surfaces colorcoded with the electrostatic potential (ESP) in Fig. 3. The states with intact polar carbonyl group, negative ESP in S_0 and $T_2(\pi, \pi^*)$, have large dipole moments. As soon as the (n,π^*) excitation redistributes the electron density from the CO group to the ring, enhancing the π-system at the double C=C bond, the dipole moments in $S_1(n, \pi^*)$ and $T_1(n, \pi^*)$ states drop significantly. This interpretation is also supported by the comparison of the IR spectra of all four states of 2CP displayed in Fig. 2. For the sake of clarity the relative intensities of the excited states were shifted by 50, 100, and 150 units. The pattern visible for S_0 and $T_2(\pi, \pi^*)$ states distinctively differs from that of $T_1(n, \pi^*)$ and $S_1(n, \pi^*)$ illustrating the presence of the double CO bond in the former pair and only partial double CO bond in the latter pair of states. The most intense IR peak for the

Fig. 3 Maps of the MP2/cc-pVTZ isodensity surface of 2-cyclopenten-1-one in its ground and excited states colorcoded with the electrostatic potential (ESP) and CCSD/Pol dipole moments

S_0 $|\mu| = 1.496$ a.u. $\quad T_2(\pi,\pi^*)$ $|\mu| = 1.124$ a.u. $\quad T_1(n,\pi^*)$ $|\mu| = 0.542$ a.u. $\quad S_1(n,\pi^*)$ $|\mu| = 0.603$ a.u.

ESP scale (a.u.): -0.06 -0.03 0.0 0.03 0.06

Table 6 Dipole polarizabilities (a.u.) of 2-cyclopenten-1-one[a]

State	Method	Basis z2Pol				Basis Pol			
		α_{xx}	α_{yy}	α_{zz}	$\overline{\alpha}$	α_{xx}	α_{yy}	α_{zz}	$\overline{\alpha}$
'Vertical'[b]									
S_0	CASSCF	55.43	41.28	75.11	57.27	56.79	42.20	75.24	58.08
	CCSD	58.12	42.30	74.44	58.29	59.66	42.80	75.93	59.46
	CCSD(T)	59.14	42.75	75.12	59.00	60.73	43.20	76.55	60.16
$S_1(n, \pi^*)$	CASSCF	58.56		74.09		61.23		77.22	
	CCSD	62.45		78.07		64.77		81.62	
$T_1(n, \pi^*)$	CASSCF	57.91	43.02	73.74	58.22	60.18	44.40	76.15	60.24
	CCSD	62.37	45.00	79.28	62.21	64.31	45.46	81.97	63.91
	CCSD(T)	63.79	45.59	80.84	63.41	65.80	45.94	83.55	65.10
$T_2(\pi, \pi^*)$	CASSCF	56.83	41.02	66.04	54.63	57.90	41.89	67.86	55.88
	CCSD	62.12	43.70	73.96	59.93	62.87	43.99	75.51	60.79
	CCSD(T)	63.11	44.09	75.45	60.88	64.16	44.02	77.51	61.90
'Adiabatic'[c]									
$S_1(n, \pi^*)$	CASSCF	59.87		67.36		61.13		69.37	
	CCSD	60.80		74.39		62.54		76.66	
$T_1(n, \pi^*)$	CASSCF	59.47	42.83	69.45	57.25	60.83	44.00	71.34	58.73
	CCSD	60.63	44.78	76.44	60.62	62.38	45.22	78.48	62.03
	CCSD(T)	61.61	45.32	77.93	61.62	63.27	45.78	80.33	63.13
$T_2(\pi, \pi^*)$	CASSCF	53.62	44.30	62.12	53.35	55.12	45.31	63.27	54.57
	CCSD	58.56	47.49	69.11	58.38	59.66	47.98	69.56	59.07
	CCSD(T)	59.75	48.29	71.37	59.80	60.96	48.92	71.25	60.38

[a] MP2/cc-pVTZ geometries used, 1 a.u. = $1.648777.10^{-41}$ $C^2m^2J^{-1}$
[b] Geometries of the ground state
[c] Geometries of the given state

$T_2(\pi, \pi^*)$ state ($\sim$2120 cm^{-1}) indicates even the shortened (stronger) double CO bond.

Calculated dipole polarizabilities are presented in Table 6. We were unable to calculate the α_{yy} component of the polarizability for the $S_1(n, \pi^*)$, due to the CASSCF convergence problem with the second singlet root in the C_1 symmetry. Differences between z2Pol and Pol polarizabilities are even smaller than for dipole moments. Differences between 'vertical' and 'adiabatic' polarizabilities for $S_1(n, \pi^*)$ and $T_1(n, \pi^*)$ states are similar to differences for dipole moments, however, the difference for the $T_2(\pi, \pi^*)$ state is much smaller. All three excited states have only slightly larger polarizabilities than the ground states, these changes are considerably smaller than they were for dipole moments. Certainly, the molecule is substantially larger than H_2O or H_2S, where changes in polarizabilities for excited states were much larger [43]. Nevertheless, similar to dipole moments, we can divide the four investigated states into two classes. The first one, S_0 and $T_2(\pi, \pi^*)$, have slightly lower values of the polarizability than the second one with (n, π^*) excitations.

Conclusion

A detailed study of rotational constants, vibrational frequencies, excitation energies, dipole moments and dipole polarizabilities of the four low–lying electronic states of 2–cyclopenten–1–one has been presented. Electron correlation effects which are essential in the case of accurate calculations were accounted for by CCSD and CCSD(T) methods.

It has been shown that vertical excitation energies are in the order $T_1(n, \pi^*)$, $S_1(n, \pi^*)$ and $T_2(\pi, \pi^*)$. The order of adiabatic excitation energies is different. Triplets $T_1(n, \pi^*)$ and $T_2(\pi, \pi^*)$ are very close to each other and it is impossible for us to give a definite answer to the order question. In the cc-pVTZ basis we got the $T_1(n, \pi^*)$ state lower than $T_2(\pi, \pi^*)$, while in larger cc-pVQZ it is just opposite. The singlet $S_1(n, \pi^*)$ is well above both triplets.

The (n, π^*) excitations lead to a significant reduction of the dipole moment, while the (π, π^*) excitation reduced it much less. Interestingly, dipole moments of almost isoenergetic triplets $T_1(n, \pi^*)$ and $T_2(\pi, \pi^*)$ at the CCSD(T)/Pol level are 0.551 a.u. and 1.124 a.u., respectively. This is caused by striking differences in valence electron densities as demonstrated in Fig. 3.

Dipole polarizabilities of higher states of 2CP are much less affected by electron excitations than dipole moments. However, we can notice certain similarities in behavior of dipole moments and polarizabilities. Values for $S_1(n, \pi^*)$ and $T_1(n, \pi^*)$ are closer each to other and the same applies for S_0 and $T_2(\pi, \pi^*)$.

All the properties calculated in this study show sound trends: lower dipole moments, higher polarizabilities and the weakening of the α,β-unsaturated carbonyl bond indicate the lowering of the biological activity of 2CP in the $S_1(n, \pi^*)$ and $T_1(n, \pi^*)$ states. In this context, the activity of 2CP in the $T_2(\pi, \pi^*)$ state seems to be marginal because the $T_2(n, \pi^*) \leftarrow S_0$ transition is strongly spin–forbidden.

References

1. Steimle TC, Frey S, Le A, DeMille D, Rahmlow DA, Linton C (2011) Phys Rev A 84:012508
2. Frey SE, Steimle TC (2011) Chem Phys Lett 512:21
3. Bublitz GU, Boxer SG (1997) Annu Rev Phys Chem 48:213
4. Boxer SG (2009) J Phys Chem B 113:2972
5. Pašteka LF, Meličerčík M, Neogrády P, Urban M (2012) Mol Phys. doi:10.1080/00268976.2012.668970
6. Chao TH, Laane J (1973) J Mol Spectrosc 48:266
7. Cheatham CM, Laane J (1991) J Chem Phys 94:5394
8. Cheatham CM, Laane J (1991) J Chem Phys 94:7734
9. Ruoff R, Krebs A, Schaeffler T, Stiegler G, Bodenseh HK (1997) J Mol Struct 407:93
10. Pillsbury NR, Choo J, Laane J, Drucker S (2003) J Phys Chem A 107:10648
11. Pillsbury NR, Zwier TS, Judge RH, Drucker S (2007) J Phys Chem A 111:8357
12. Froese RDJ, Morokuma K (1996) Chem Phys Lett 263:393
13. Sunoj RB, Lakshminarasimhan P, Ramamurthy V, Chandrasekhar J (2001) J Comput Chem 22:1598
14. Garcia-Exposito E, Bearpark MJ, Ortuno RM, Branchadell V, Robb MA, Wilsey S (2001) J Org Chem 66:8811
15. Choo J, Kim S, Drucker S, Laane J (2003) J Phys Chem A 107:10655
16. Grimme S, Izgorodina EI (2004) Chem Phys 305:223
17. Rossi A, Elia G, Santoro MG (1996) J Biol Chem 271:32192
18. Ianaro A, Maffia P, Cuzzocrea S, Mazzon E, Santoro MG, Di Rosa M, Ialenti A (2003) FEBS Lett 553:21
19. Rosetri M, Frasnelli M, Fabbri F, Arienti C, Vannini I, Tesei A, Zoli W, Conti M (2008) Anticancer Res 28:315
20. Roberts SM, Santoro MG, Guyot T (1999) J Chem Soc Perkin Trans 1:2437
21. Tian JA, Li DL, Zhai FY, Wang XH, Li R (2010) Med Chem Res 19:1162
22. Cai X-H, Xie B (2011) Res J Chem Sci 1:120
23. Frisch MJ, Trucks GW, Schlegel HB, Scuseria GE, Robb MA, Cheeseman JR, Montgomery JA, Vreven T, Kudin KN, Burant JC, Millam JM, Iyengar SS, Tomasi J, Barone V, Mennucci B, Cossi M, Scalmani G, Rega N, Petersson GA, Nakatsuji H, Hada M, Ehara M, Toyota K, Fukuda R, Hasegawa J, Ishida M, Nakajima T, Honda Y, Kitao O, Nakai H, Klene M, Li X, Knox JE, Hratchian HP, Cross JB, Bakken V, Adamo C, Jaramillo J, Gomperts R, Stratmann RE, Yazyev O, Austin AJ, Cammi R, Pomelli C, Ochterski JW, Ayala PY, Morokuma K, Voth GA, Salvador P, Dannenberg JJ, Zakrzewski VG, Dapprich S, Daniels AD, Strain MC, Farkas O, Malick DK, Rabuck AD, Raghavachari K, Foresman JB, Ortiz JV, Cui Q, Baboul AG, Clifford S, Cioslowski J, Stefanov BB, Liu G, Liashenko A, Piskorz P, Komaromi I, Martin RL, Fox DJ, Keith T, Al-Laham MA, Peng CY, Nanayakkara A, Challacombe M, Gill PMW, Johnson B, Chen W, Wong MW, Gonzalez C, Pople JA (2004) Gaussian 03, Wallingford, CT
24. Aquilante F, De Vico L, Ferré N, Ghigo G, Malmqvist PÅ, Neogrády P, Pedersen TB, Pitoňák M, Reiher M, Roos BO, Serrano-Andrés L, Urban M, Veryazov V, Lindh R (2010) J Comput Chem 31:224-247
25. Roos BO, Taylor PR, Siegbahn PEM (1980) Chem Phys 48:157
26. Urban M, Černušák I, Noga J Kellö V (1987) In: Wilson S (ed) Methods in computational chemistry, vol 1. Plenum, New York, p 117
27. Bartlett RJ (1995) In: Yarkony DR (ed) Advanced Series in Physical Chemistry, vol 2. World Scientific, Singapore, p 1047
28. Neogrády P, Szalay PG, Kraemer WP, Urban M (2005) Collect Czech Chem Commun 70:951
29. Dunning TH (1989) J Chem Phys 90:1007
30. Sadlej AJ (1988) Collect Czech Chem Commun 53:1995
31. Sadlej AJ (1991) Theor Chim Acta 79:123
32. Černušák I, Kellö V, Sadlej AJ (2003) Collect Czech Chem Commun 68:211
33. Benková Z, Sadlej AJ, Oakes RE, Bell SEJ (2005) J Comput Chem 26:145
34. Iliaš M, Kellö V, Urban M (2010) Acta Phys Slovaca 60:259
35. Cohen HD, Roothaan CC (1965) J Chem Phys 43:S34
36. McLean AD, Yoshimine M (1967) J Chem Phys 46:3682
37. Černušák I, Diercksen GHF, Sadlej AJ (1986) Phys Rev A 33:814
38. Jacquemin D, Champagne B, André JM (1997) Int J Quantum Chem 65:679
39. Maroulis G (1998) J Chem Phys 108:5432
40. Sagear P, Laane J (1995) J Chem Phys 102:7789
41. NIST/EPA Gas-Phase Infrared Database, http://webbook.nist.gov/chemistry/form-ser.html, retrieved August 29, 2011
42. Irikura KK, Johnson RD, Kacker RN, Kessel R (2009) J Chem Phys 130:114102
43. Paleniková J, Kraus M, Neogrády P, Kellö V, Urban M (2008) Mol Phys 106:2333